

RF coupling impedance measurements versus simulations

A. Mostacci*, L. Palumbo, Università La Sapienza, Roma, Italy
B. Spataro, LNF-INFN, Frascati, Italy,
F. Caspers, CERN, Geneva, Switzerland.

Abstract

Bench measurements nowadays represent an important tool to estimate the coupling impedance of any particle accelerator device. The well-known technique based on the coaxial wire method allows to excite in the device under test a field similar to the one generated by an ultra-relativistic point charge. Nevertheless the measured impedance of the device needs comparisons to numerical simulations and, when available, theoretical results. We discuss the basics of the coaxial wire method and report the formulae widely used to convert measured scattering parameters to longitudinal and transverse impedance data. We discuss typical measurement examples of interest for the LHC. In case of resonant structures, impedance measurements and comparison with simulations become easier. The bead-pull technique may be used in this case.

INTRODUCTION

The interaction between a (relativistic) beam and its surroundings is usually described in terms of longitudinal and transverse coupling impedance [1]. The longitudinal impedance accounts for the energy lost by a point charge q because of the wake field of a leading particle; assuming an infinitely long pipe, for a relativistic beam it is defined as

$$Z_{\parallel}(\omega) = -\frac{1}{q} \int_{-\infty}^{\infty} E_z(r=0; \omega) \exp\left(j\frac{\omega}{c}z\right) dz, \quad (1)$$

where E_z is the longitudinal electric field and c is the speed of light. Instead the transverse kick experienced by a particle because of deflecting fields excited by a leading charge, can be described in terms of the transverse coupling impedance

$$Z_{\perp}(\omega) = \frac{j}{q^2} \int_{-\infty}^{\infty} \frac{F_{\perp}(r_1, r_2; \omega)}{r_1} \exp\left(j\frac{\omega}{c}z\right) dz, \quad (2)$$

where F_{\perp} is the transverse Lorentz force and r_1 (r_2) is the leading (trailing) particle position. Longitudinal impedance is, therefore, measured in Ω while the transverse one in Ω/m .

Often beam dynamics in circular machines is studied in the frequency domain due to the intrinsic periodicity and then coupling impedances are used to estimate the effect of any accelerator device on the beam stability. Coupling impedance is then an important design parameter for any element to be installed in the machine. In the LHC case, the impedance of most elements is carefully

optimized through numerical simulations, bench measurements and confirmed by beam measurements, when available. Coupling impedance data of each LHC device could be stored in a database to eventually compute bunch instability thresholds for any possible machine settings [2].

In the design stage, coupling impedance can be estimated either by numerical simulations or by bench measurements. Nowadays numerical simulations greatly exploit commercial general purpose codes solving Maxwell equations in the Device Under Test (DUT), i.e. computing the electromagnetic field in any point of the structure (3D simulations). Time domain codes exist (MAFIA [3] and GdfidL [4]) directly providing wake-potentials which can be Fourier transformed to get coupling impedances. Other general purpose codes can be, as well, used to estimate coupling impedance of any DUT by simply simulating the bench measurement discussed below; for example that is the case of HFSS [5] (frequency domain) or MWstudio [3] (time domain). Less general codes, studying EM fields in symmetric (2D) structures (e.g. SUPERFISH [6] or OSCAR2D [7]) are used as well. There exist also “dedicated” codes which compute only the longitudinal and transverse coupling impedances of 2D structures in a very reliable way; the most famous is ABCI [8]. Numerical codes computing coupling impedances in specific geometries have also been developed, but they will not be discussed here.

The aim of this paper is to briefly review the standard way of bench measuring coupling impedances and to discuss comparisons with numerical simulation, through some meaningful examples. The coaxial wire method is the most well known bench method and it is firstly discussed for longitudinal and transverse impedance measurement. The wire set-up can also be used to study the properties of the structure when excited by a beam passing through; trapped modes or beam transfer impedance can, for example, be measured in this way. Impedances in resonant structures (e.g. accelerating or deflecting cavities) deserve a different treatment and they are measured with bead-pull techniques, discussed in a later section. Throughout the paper, we will try to discuss the agreement between measurement and simulations in typical cases, pointing out some open questions as well.

THE COAXIAL WIRE METHOD

Motivation and validation

The field of a relativistic point charge q in the free space (or in a perfectly conducting beam pipe) is a Transverse Electric Magnetic (TEM) wave; namely it has only compo-

* Andrea.Mostacci@uniroma1.it

nents transverse to the propagation direction (z -axis):

$$E_r(r, \omega) = Z_0 H_\varphi(r, \omega) = \frac{Z_0 q}{2\pi r} \exp\left(-j\frac{\omega}{c}z\right), \quad (3)$$

being E_r (H_φ) the electric (magnetic) radial (azimuthal) field component. The amplitude scales inversely with the distance r from the propagation axis and the propagation constant is ω/c . The fundamental mode of a coaxial waveguide is a TEM wave as well, with the same amplitude dependence on $1/r$ and the same propagation constant. For example, let us consider a perfectly conducting cylindrical waveguide with circular cross section of radius b with a conductor of radius a on the axis of the guide. The resulting coaxial structure allows the propagation, at any frequencies, of a TEM mode whose field is given by

$$E_r(r, \omega) = Z_0 H_\varphi(r, \omega) = Z_0 \frac{A}{r} \exp\left(-j\frac{\omega}{c}z\right), \quad (4)$$

where A is a constant depending on the power actually flowing in the guide. Therefore the excitation due to a relativistic beam in a given DUT can be “simulated” by exciting a TEM field by means of a conductor placed along the axis of the structure. The impedance source on the DUT will scatter some field, i.e. exciting some higher order modes; such modes must not propagate otherwise the propagating field will not be anymore similar to the the TEM beam field. In principle, then, simulating the beam field with the TEM mode of a coaxial waveguide is possible only at frequencies below the first higher mode cut-off, namely below the TM_{01} cut-off frequency. One can also demonstrate that the modes of the coaxial waveguide converges for vanishing wire radius to the analogous mode of the cylindrical waveguide, at least at the beam pipe boundary, where the impedance source is usually located [9].

To compare the excitation of a given DUT by a coaxial wire and with the beam itself, we are going to discuss some measurements done in the framework of the investigations of the shielding properties of coated ceramic vacuum chambers [10]. The 500 MeV CERN EPA electron beam was sent through two identical ceramic vacuum chamber sections; the first one was internally coated with a layer of $1.5 \mu\text{m}$ depth (DC resistance of 1Ω). Magnetic field probes were placed to measure the beam field just outside the two ceramic chambers (the coated and the reference one). In 1999 experiment, shielding properties of the resistive coating (thinner than the skin depth) were demonstrated, confirming previous indirect measurements and simulations [11]. In the 2000 experiment, among other results, it was proved that the screening properties of the coating can be spoiled by the addition of a second conducting layer placed outside the field probes and electrically connected to the metallic vacuum chamber sections. In this case, in fact, the magnetic field probe was measuring clearly the field of the 1 ns (r.m.s.) bunched beam (see Fig. 1). The same chamber in the same configuration (i.e. with this additional external conductor) was then measured in the bench set-up: a 0.8 mm diameter wire was stretched

on the axis of the structure. One end of the wire was connected to a 50Ω load while the other end was connected to one port of a Vector Network Analyzer (VNA); matching resistors were used. The other port of the VNA was connected to the field probe. The network analyzer was set to send through the wire a synthetic pulse (time domain option) with 300 MHz bandwidth and measured the transmission between the ports, i.e. the signal through the probe. This particular kind of set-up is not very often used, but it is very similar to the “time domain” measurement originally proposed by Sands and Rees in the 70s’ [12]; nowadays time domain measurements are often performed with synthetic pulse techniques in many microwaves applications. The measurement with the beam and with the wire should give virtually the same result, apart from a scaling factor due to the difference of the power carried by the beam and by the VNA signal. The results are shown in Fig. 1 where the beam and the bench data have been normalized and time shifted so that the traces coincides in their minimum point. The external shield, having a DC resistance much smaller than the coating, carries the image currents, the field penetrates the ceramic and the field probe can measure a clear signal. This is only one of the configurations measured both with the beam and in the bench set-up; the agreement with other measurements is similar to the one of Fig. 1. The results of that comparison confirm the validity of the coaxial wire approach to simulate the beam field effect on a given DUT.

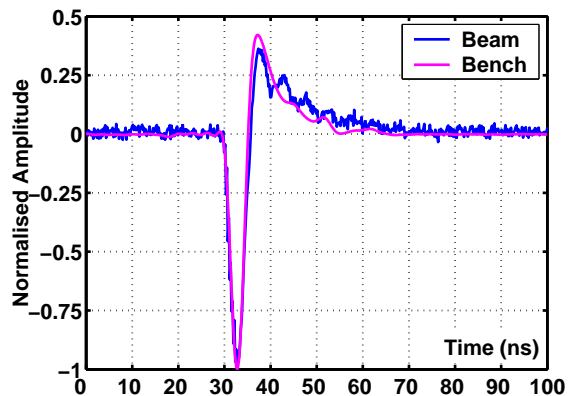


Figure 1: Signal from the field probe after normalization and time shifting in the EPA experiment on coated chamber shielding properties. The field probe is inserted between the coated ceramic and an external conductor connected to the beam pipe.

The coaxial wire bench measurement exploits the analogy between a relativistic point charge field and the fundamental mode of a coaxial waveguide. Therefore a metal wire is stretched in the DUT which is then transformed in a coaxial transmission line. Thus the longitudinal coupling impedance can be inferred from the properties of such a transmission line, provided that only the (fundamental) TEM mode is propagating. To bench measure longitudinal

impedance, a wire along the axis of the structure is needed, while transverse impedance can be measured from a single displaced wire or two wires placed symmetrically with respect to the axis. A detailed review of the method, including some practical measurement tips, can be found in Ref. [13].

Longitudinal Coupling Impedance

The wire stretched in the DUT of length L can be modeled, as mentioned before, as a TEM coaxial line of length L . In general, such a line is considered to have distributed parameters but in case of L much smaller than the wavelength λ the lumped elements approximation is applicable. The DUT beam coupling impedance is then modeled as a series impedance of an ideal reference line (REF). Therefore coupling impedance can be obtained from the REF and DUT characteristic impedances and propagation constants of the lines (see for example Ref. [14]). It is well known that any transmission line can be characterized by measuring its scattering S -parameters, for example with VNA. In principle both reflection (i.e. S_{11}) and transmission measurement (i.e. S_{12}) are possible, but usually transmission measurement are preferred for practical reasons. In the framework of this transmission line model, the DUT coupling impedance can be exactly computed from measured S -parameters but the procedure is cumbersome and not practically convenient. Therefore a number of approximated formulae are derived in literature and we will report the most used ones, highlighting their approximations. All the following formulae do not consider the effect of the mismatch at the beginning and at the end of the perturbed transmission line. Therefore matching networks (resistive networks or cones) are normally used in the actual bench set-ups. Cones are mechanically difficult and act as a frequency dependent distributed transformer which doesn't work at low frequency; on the contrary resistive networks are affected by parasitic inductances and capacitances affecting their performance at high frequency (depending on the components actually used). Approximated formulas and the "exact" transmission line solution are numerically compared in Ref. [15].

Being Z_c the characteristic impedance of the wire inside the DUT, the beam coupling impedance $Z_{||}$ can be estimated with the "improved log-formula" [14]

$$Z_{LOG} = -Z_c \ln \left(\frac{S_{21}^{DUT}}{S_{21}^{REF}} \right) \left[1 + \frac{\ln(S_{21}^{DUT})}{\ln(S_{21}^{REF})} \right]. \quad (5)$$

Expressing the S_{21}^{REF} in terms of the DUT electrical length L one can get another equation analogous to Eq. (5) [16]:

$$Z_{LOG} = -Z_c \ln \left(\frac{S_{21}^{DUT}}{S_{21}^{REF}} \right) \left[1 + \frac{jc}{2\omega L} \ln \left(\frac{S_{21}^{DUT}}{S_{21}^{REF}} \right) \right], \quad (6)$$

which can be useful in practice. The improved impedance expression requires the knowledge of the electrical length

of the DUT and its accuracy decreases for shorter devices [17]. Reference [15] suggests the use of improved log-formula for DUT longer than the wavelength λ .

For small ratios $Z_{||}/Z_c$, the so called "standard log-formula" has been proposed for the distributed impedances [18]:

$$Z_{log} = -2Z_c \ln \left(\frac{S_{21}^{DUT}}{S_{21}^{REF}} \right). \quad (7)$$

The log-formula Eq. (7) is generally applicable including lumped components, provided that no strong resonance is present and the perturbation treatment is justified.

For lumped elements, i.e. when the DUT electric length is much smaller than the wavelength, the previous expressions converge to the so called "lumped element formula" [19]:

$$Z_{HP} = -2Z_c \frac{S_{21}^{DUT} - S_{21}^{REF}}{S_{21}^{DUT}}. \quad (8)$$

The lumped impedance formula is applicable to single resonances and has the advantage that the scattering coefficient ratio is directly converted into an impedance by the network analyzer [20].

The quantities Z_{LOG} , Z_{log} , Z_{HP} are estimations of the beam coupling impedance $Z_{||}$; the smaller the ratio $Z_{||}/Z_c$, the more accurate are the approximated formulae. As an example, a wire in a perfectly conducting cylindrical beam pipe with circular cross section has a characteristic impedance equal to

$$Z_c = \frac{Z_0}{2\pi} \ln \left(\frac{b}{a} \right) \quad (9)$$

where a is the wire radius, b is the (inner) pipe radius and Z_0 is the vacuum impedance. Therefore a smaller wire has an higher Z_c , resulting in a more accurate measurement of the coupling impedance. A detailed discussion of the systematic error done in estimating the beam coupling impedance $Z_{||}$ with Z_{LOG} , Z_{log} or Z_{HP} is reported in Ref. [17].

The difference between the improved log formula Eq.s (5, 6) and the standard one Eq. (7) can be shown in measurements performed on the 7 cells module of the MKE kicker [23]. The coupling impedance is much bigger than the characteristic impedance of the wire in the DUT ($\approx 300\Omega$) and therefore the improved log formula must be used:

$$Z_{LOG} = Z_{log} \left[1 + \frac{jc}{2\omega L_f} \ln \left(\frac{S_{21}^{DUT}}{S_{21}^{REF}} \right) \right]. \quad (10)$$

Equation (10) differs from Eq. (6) because the length of the ferrite ($L_f = 1.66\text{m}$) is used instead of the length of the whole kicker tank ($L = 2.31\text{m}$), as discussed in Ref. [23]. Figure 2 shows the wire measurement results interpreted with the improved formula Eq. (10) (green line) and the standard one Eq. (7) (blue line). The comparison with theory (black line) shows that, at least for the

real part of the impedance, the improved log formula gives a result closer to theoretical expectations for frequencies higher than few hundreds of MHz. At lower frequencies, i.e. where the DUT length is comparable to the wavelength and the impedance is much closer to the characteristic impedance of the wire in the DUT, the standard log formula is a better estimation of the coupling impedance.

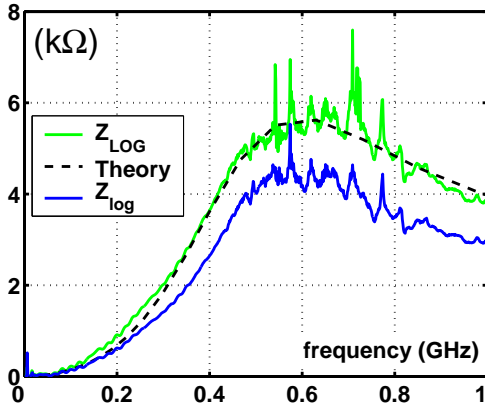


Figure 2: Real part of the longitudinal coupling impedance for the 7 cells MKE kicker module [23]. The measured data are interpreted via the improved log formula (green line) or the standard log formula (blue line) and compared to theoretical expectations (dashed line).

As an example of a comparison between numerical simulation and bench measurement of longitudinal coupling impedance, we briefly discuss the case of the LHC injection kicker. In particular, to study the impedance of the LHC injection kicker a 1 meter long model has been built and bench measured [21]; the measured impedance data have been also compared to HFSS simulations [22].

The model consists of a ceramic test chamber (shown in Fig. 3) with 30 printed conducting strips inside; the strips have different widths and are done using the same technology of the final LHC kicker. Good RF-contacts are assured on either side (“A” and “C” in Fig. 3). The lower part (rectangular steel profile underneath the ceramic tube) serves both as mechanical support and as electrical simulation for the “cold conductor” of the kicker. The “printed” coupling capacitor is visible near the right connector (position “C”) and has pyramid like “teeth” toward position “B”. These “teeth” are intended as an RF match (gradual transition for the image current) toward higher frequencies. A coaxial Cu-Be wire is stretched on the axis of the structure and it is soldered through matching resistors to the two RF connectors in each side of the chamber. Such a bench measurement set-up has been simulated with HFSS, including the current bypass conductor, but with 12 identical strip lines of the same width to avoid complexity [22].

We refer for the details of the measurement to Ref. [21] and for the simulation to Ref. [22], where more extensive explanations can be found. The coupling impedance ex-

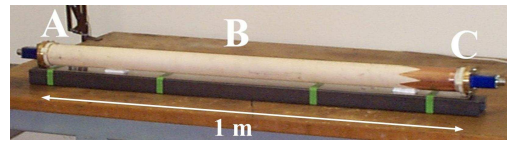


Figure 3: Model for the LHC injection kicker [21].

hibits some peaks at particular frequencies being negligible in all the rest of the measured frequency range. To compare measurement and simulations, we have reported in Table 1 the values of the main peaks of the longitudinal coupling impedance measured with the wire bench set-up and estimated with the HFSS simulation of the wire measurement itself. The agreement between measurement and simulations shown in Table 1 is satisfactory considering that only 12 over 30 conducting strips are included in the simulations, which essentially explains the difference.

Table 1: Impedance measurements and simulations for the model of the LHC injection kicker.

Simulations [22]		Measurements [21]	
Freq. (MHz)	Z_{\parallel} (Ω)	Freq. (MHz)	Z_{\parallel} (Ω)
14	500	17	700
28	44	31	121
410	65	442	163
810	40	846	60

According to Ref. [22], the origin of the 17 MHz peak is the resonance of the capacitor at one end and the inductance created by the strips and the outer support. To damp this low frequency resonance a lossy ferrite ring was inserted; measurements and simulations agree in estimating a reduction of the amplitude of the impedance. The 31 MHz peak is mainly due to a transverse resonance and it is very much affected by an imperfectly tightened wire or by a small offset of the wire itself. In the simulations [22] this resonance is practically canceled with a 2 mm offset of the wire; measurements give similar results [21]. The origin of the 442 MHz and of the 846 MHz peaks is by the coaxial waveguide resonance at the copper tape (point “C” in Fig. 3).

In conclusion, longitudinal coupling impedance bench measurements are reasonably well understood and the technique is well established. With modern simulation codes, one can derive directly the coupling impedance or simulate the bench set-up with wire, virtually for any structure. Evaluation of coupling impedance from measured or simulated wire method results require the same cautions; but simulations and RF measurements usually agree well. Moreover comparison with numerical results are very useful to drive and to interpret the measurements. One should pay attention that simulation may require a simplified DUT model which will only reproduce the main DUT electro-

magnetic features.

Transverse Coupling Impedance

The transverse impedance is proportional at a given frequency to the change in longitudinal impedance due to the lateral displacement of the beam in the plane under consideration (vertical or horizontal). Therefore the transverse impedance is proportional to the transverse gradient of the longitudinal impedance (Panowsky-Wentzel theorem [1]).

Based on this theorem, the most common method to bench measure transverse impedance uses two parallel wires stretched along the DUT [13]. Opposite currents are sent through the wires (odd mode excitation); instead of the wires, a loop can be used to increase signal to noise ratio [25]. The bench transverse impedance $Z_{\perp,bench}$ is given by [24]

$$Z_{\perp,bench} = \frac{Z_{\parallel,bench}c}{\omega\Delta^2}, \quad (11)$$

where Δ is the wire spacing (usually about 10% of the DUT radius). $Z_{\parallel,bench}$ is the longitudinal coupling impedance measured from the S -parameters as discussed above, e.g. using the improved log-formula

$$Z_{\perp,LOG} = -\frac{Z_c c}{\omega\Delta^2} \ln\left(\frac{S_{21}^{DUT}}{S_{21}^{REF}}\right) \left[1 + \frac{\ln(S_{21}^{DUT})}{\ln(S_{21}^{REF})}\right],$$

where now Z_c is the characteristic impedance of the odd mode of a two wires transmission line. Concerning LHC (and other future machines as well), low frequency transverse impedance is interesting and therefore the lumped element Eq. (8) must be used in Eq. (11). A practical example of low frequency transverse impedance is reported in Ref. [25] for a simple case; results are compared to theoretical expectations to define a reliable measurement procedure.

In the two wires bench set-up only dipole field components are excited because of the symmetry of the wires/coil; therefore there is no electric field component on the axis. In numerical simulations, this is analogous to putting a metallic image plane between the wires. Nevertheless some accelerator devices may exhibit a strong asymmetry in the image current distribution due to azimuthal variation of conductivity (e.g. ferrite in kickers) or to cross section shape. Two wire techniques can be used with some cautions in this cases because the field in the structure is not TEM-like; in order to get a more complete view of the transverse kick on the beam, it may be useful to characterize the device with a single wire [26].

The transverse impedance itself can be measured with a single wire displaced in various positions, that is measuring the longitudinal coupling impedance as a function of the displacement x_0 of a single wire. From the Panowsky-Wentzel theorem we get

$$Z_{\perp,bench} \simeq \frac{c}{\omega} \frac{Z_{\parallel,bench}(x_0) - Z_{\parallel,bench}(x_0 = 0)}{x_0^2},$$

provided that x_0 is small with respect to the typical variation length of the bench measured coupling impedance $Z_{\parallel,bench}$.

From the practical point of view, transverse impedance measurement techniques are more delicate and require particular attention for asymmetric devices (e.g traveling wave kickers like). Novel techniques optimized for particular DUTs, are also being proposed, e.g. SNS kicker measurements reported in Ref. [27]. Numerical simulations are necessary to control and validate the measurement procedure. One should pay attention that DUT models feasible for simulations do not introduce non physical symmetries or approximations; in principle, dealing with transverse problem may require more complex simulations than the longitudinal case.

Other applications: trapped mode finding

A coaxial wire set-up can also be used to study the behavior of a given DUT when traversed by a relativistic beam. For instance, it can be useful to measure the beam transfer impedance or to check if trapped mode are excited in a given structure. The beam transfer impedance is the ratio between a voltage signal induced because of the beam structure interaction and the beam current. Examples of beam transfer impedance for a bunch length monitor is reported in Ref.s [29, 30], while we are going to discuss briefly how a coaxial wire set-up has been used to study the possibility of trapped modes in the LHC recombination chamber.

In the LHC interaction regions, the separated beam pipes join in a common region to allow collisions. Thus the beam “sees” an enlargement of the beam pipe that, if not properly tapered, can lead to trapped modes dangerous for the beam stability. Such modes exist in the LHC chambers, but luckily enough they are too weak to affect the beam stability. To prove it, numerical simulations and bench measurements were done as reported in Ref. [28] and related references where the interested reader can find additional details. In the following we report part of that work, in particular focusing on comparisons between measurements and simulations.

A simplified (rectangular and scaled) model of the recombination chamber was built to be bench measured with a coaxial wire set-up. In the original design the transition is tapered; in our model the taper was first removed to prove the existence of the trapped mode and then added again to show the reduction of the mode amplitude.

To demonstrate the feasibility of the measurement, HFSS simulations were done and the results are shown in Fig. 4. Picture a) of Fig. 4 shows the electric field at 2.737 GHz: the trapped mode at the wedge is excited and there is no transmission along the wire: the signal is reflected and one can see a stationary wave pattern of the field. Picture b) of Fig. 4 shows that at other frequencies (e.g. 2.5 GHz) the field is confined around the wire but can propagate from one end of the wire to the other. There-

fore, the HFSS simulations show that the trapped mode is present and that it can be measured by looking for a strong notch in the transmission coefficient between the two ends of the wire.

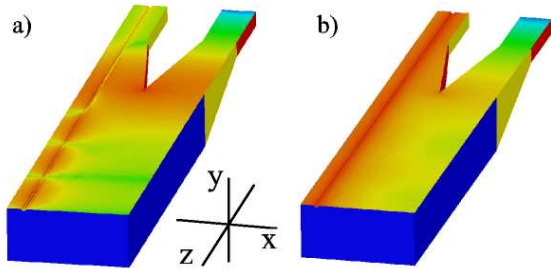


Figure 4: Amplitude of the electric field (maximum value) for the bench set-up of the LHC recombination chamber at 2.737 GHz (left plot) and 2.5 GHz (right plot) by HFSS simulations.

The same geometry, i.e. without tapering, have also been simulated with MAFIA, i.e. computing directly wake potentials. The result for the real part of the coupling impedance Z_{RE} is shown in Fig. 5. The strong peak at 2.800 GHz is due to the trapped mode.

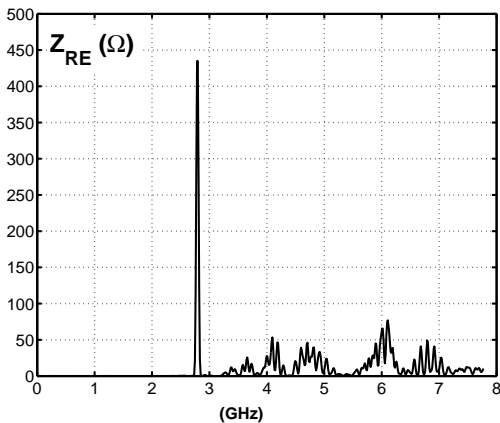


Figure 5: Real part of the longitudinal coupling impedance for the bench set-up of the LHC recombination.

Measurements of the transmission between the ends of the wire are shown in Fig. 6 in terms of the transmission scattering parameter S_{12} . As expected, there is a strong notch at 2.753 GHz where the trapped mode is excited and the electromagnetic power remains confined in the structure.

Additional measurements and MAFIA simulations have been done including a taper resembling the actual geometry of the recombination chamber. The beneficial effect of reducing the trapped mode has been shown both from measurement and from simulations [28].

Thus also in this case, measurements and simulations give close results. It is worth noticing that while HFSS

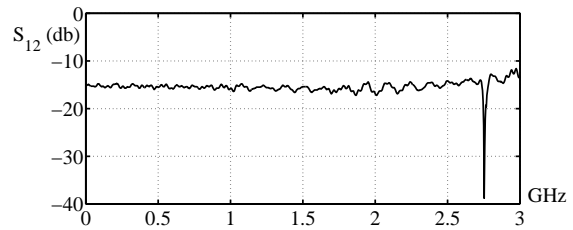


Figure 6: Transmission coefficient between the two ends of the wire in the the bench set-up of the LHC recombination.

gives actually simulations of the bench measurement, MAFIA simulations compute directly the wakefields, that is the structure is “excited” directly by a particle beam; the agreement of the results, therefore, assesses the coupling impedance measurement and computation techniques.

RESONANT STRUCTURES

An important class of accelerator devices are cavities which are now used both for accelerating and deflecting the particle beam. Each cavity is characterized by its resonant frequency f_0 , the quality factor of the resonance Q and its shunt impedance R . One can think of measuring all these quantities with the coaxial wire set-up, i.e. measuring strong notches in the transmission scattering coefficient between the ends of the wire. But the wire perturbs longitudinal cavity modes, e.g. lowers the Q and detunes the frequency. Therefore the coaxial wire set-up is not usually recommended for cavity measurements and it is advisable only for special cases, mainly transverse modes [13].

The most used technique to characterize cavities is the “bead pull” measurement [31]. The field in the cavity can be sampled by introducing a perturbing object and measuring the change in resonant frequency: where the field is maximum (minimum) the resonance frequency will be more (less) perturbed. It is a perturbation method, therefore the perturbing object must be so small that the field does not vary significantly over its largest linear dimension. Shaped beads are used to enhance perturbation and give directional selectivity among different field components.

Quantitatively, the change of the resonant frequency is related to the perturbed cavity field by the Slater theorem. For the typical case of longitudinal electric field on the axis of accelerating cavities, the variation of the resonance frequency Δf from the unperturbed one is [32]

$$\frac{\Delta f}{f_0} = -\Delta V \varepsilon_0 k_E \frac{E_z^2}{4U}$$

for a conducting bead of volume ΔV ; E_z is the field at the perturber position and U is the electromagnetic energy stored in the cavity. The form factor k_E of the the perturbing object can be exactly calculated for ellipsoids or can be calibrated in a known field (e.g. TM_{0n0} of a pillbox cavity).

The frequency variation can be measured by the variation of the phase ϕ at the unperturbed resonant frequency,

according to [33]

$$\frac{\Delta f}{f_0} = \frac{\tan \phi(f_0)}{2Q_L} \simeq \frac{\phi(f_0)}{2Q_L}$$

where Q_L is the (loaded) quality factor of the resonance. Even if a very precise initial tuning is needed, this method allows easily measuring the field of many points (as many as the points of the instrument trace). The field shape can also be directly visualized on the instrument screen, greatly facilitating the structure tuning procedure.

As an example we can consider simulations and measurements done on an 11.424 GHz standing wave multi-cell cavity, designed for the SPARC project [34]. The cavity is supposed to work in the π -mode (all the cells are filled with field) exhibiting a maximum field equal in every cell (field flatness). A 9 cells prototype has been designed and built and all the details are reported in Ref. [34] while a picture is given in Fig. 7.

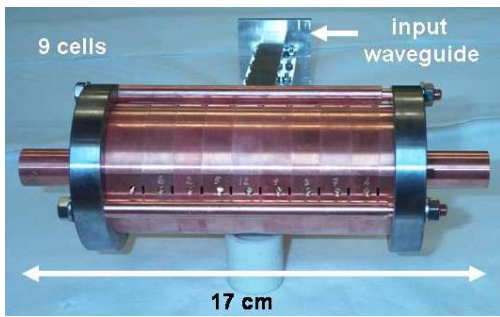


Figure 7: Nine cells copper prototype of the SPARC 11 GHz cavity.

Figure 8 compares measured data against numerical simulation results for the electric field on axis. The field has a maximum/minimum in the center of every cell and the tuners have been set to have the required field flatness. The main measurement artifact was the non-negligible effect of the glue used to fix the bead on a plastic wire to be moved by the stepping motor; therefore the glue effect was measured and calibrated away resulting in the data reported in Fig. 8. Numerical codes gives very close results among each other and they all agree well with measurements.

An important cavity design parameter is the R/Q which can be obtained from electric field data using

$$\frac{R/Q}{L_c} = \frac{1}{U\omega L_c} \left| \int_0^{L_c} E_z(z) \exp\left(j\frac{\omega}{c}z\right) dz \right|^2, \quad (12)$$

where L_c is the length of the structure. From measurement and simulations we get the results given in Table 2 which again shows the good agreement among measurements and simulations. The number in round brackets is the uncertainty of the measurement according to the procedure given in Ref. [35] (Type A evaluation).

In general measurement on resonant structures are accurate and in very good agreement with simulations. Bead

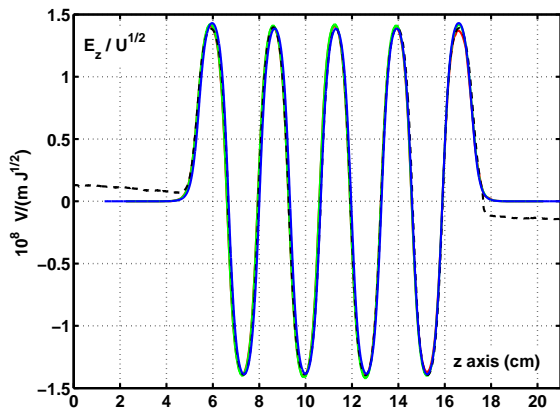


Figure 8: Longitudinal electric field on the SPARC cavity axis: HFSS simulations (red line), SUPERFISH simulations (green line), MAFIA simulations (blue line) and bead pull measurements (black dashed line).

Table 2: SPARC 11 GHz cavity: R/Q per unit length.

	HFSS	SUPERFISH	MAFIA	Meas.
Ω/m	9138	9232	9392	9440(87)

pull measurements are often used to check if the DUT fits the design specifications and they are still required for tuning the multiple cell cavities. R/Q measurements agree always very well with simulations (within the 3%).

CONCLUSIONS AND OUTLOOK

The most common bench methods for measuring coupling impedance have been discussed: wire method (longitudinal and transverse impedance) and bead pull method (resonant structures). There are several codes usable to estimate coupling impedances (MAFIA, HFSS, GdfidL, MWstudio, ABCI, OSCAR2D, SUPERFISH). Impedance can be computed by numerical RF simulators or calculating directly the wakefields or by simulating the wire measurement. Numerical simulations often deal with simplified models: i.e. one must have some insight into the problem. With reasonable and accurate modeling, a longitudinal impedance simulation usually reproduces experimental results (and vice-versa). Transverse impedance requires a much deeper control of both simulations and bench measurements, particularly for some special devices. Impedances of resonant structures are well modeled by numerical simulation with high degree of reliability.

Transverse impedance measurements are surely more challenging than longitudinal ones for modern accelerators devices. Single moving wire techniques should surely be investigated (Panowsky-Wentzel theorem). The measurement techniques strongly depends on the device to be tested; in collimators, for example, one could keep the wire

fixed and move the collimator plates. Nowadays mechanical drawings of complex accelerator components are available in electronic CAD formats and it would be highly desirable to use them as input files of some electromagnetic field simulator. In most case only simplified schematic models of such complex geometries can be efficiently simulated (e.g. kickers). Moreover electromagnetic models of material used in some devices (e.g. special ferrite in some kickers) are still missing in certain state-of-art commercial numerical electromagnetic field simulators.

ACKNOWLEDGMENTS

The authors are grateful to F. Ruggiero and the CARE-HHH workshop organization team for the invitation to the workshop. H. Tsutsui (Sumitomo) and D. Alesini (INFN) helped a lot with fruitful discussions; T. Linnecar carefully read the manuscript giving helpful comments. The EPA experiment was organized and carried out also by L. Vos, D. Brandt and L. Rinolfi (CERN). V. Lollo, A. Bacci, V. Chimenti (INFN) are involved in the design and the prototyping of the 11 GHz cavity for SPARC. Students of the "Accelerators and detectors" laboratory at Energetics Department of Università "La Sapienza" substantially helped in setting up the bead-pull measurement for SPARC cavities.

REFERENCES

- [1] L. Palumbo, V.G. Vaccaro and M. Zobov, in *Fifth Advanced Accelerator Physics Course*, CAS Cern Accelerator School, CERN 95-06 (1995), p.331. See also INFN LNF-94/041 (1994).
- [2] O. Bruning, CERN SL-96-069-AP (1996).
- [3] <http://www.cst.com>.
- [4] <http://www.gdfidl.de>
- [5] <http://www.ansoft.com>.
- [6] I. Halbach and R. F. Holsinger, *Particle Accelerators* 7, 213-222 (1976).
- [7] P. Fernandes, R. Parodi, *IEEE Transactions on Magnetics*, vol. 27-5 (1991), pp.3860-3863.
- [8] Y. H. Chin, CERN LEP-TH/88-3 (1988).
- [9] A. Argan, Private Communication (2000).
- [10] L. Vos, F. Caspers, A. Mostacci et al., CERN AB-Note-2003-02 MD EPA (2003).
- [11] F. Caspers, E. Jensen, F. Ruggiero et al., "RF Screening by Thin Resistive Layers", PAC'99, New York (1999).
- [12] M. Sands, J. Rees, SLAC report PEP-95 (1974).
- [13] F. Caspers in *Handbook of Accelerator Physics and Engineering*, A. Chao and M. Tinger (editors), World Scientific, Singapore (1998), p.570.
- [14] V.G. Vaccaro, INFN/TC-94/023 (1994).
- [15] E. Jensen, CERN PS/RF/Note 2000-001 (2000).
- [16] F. Caspers, C. Gonzalez, M. Dyachkov, E. Shaposhnikova, H. Tsutsui, CERN PS/RF/Note 2000-004 (2000).
- [17] H. Hahn, *Phys. Rev. ST Accel. Beams* 3, 122001 (2000).
- [18] L. Walling et al, NIM A281 (1989), p.433.
- [19] H. Hahn, F. Pedersen, BNL50870 (1978).
- [20] H. Hahn, *Phys. Rev. ST Accel. Beams* 7, 012001 (2004).
- [21] F. Caspers, A. Mostacci, CERN PS/RF/Note 2002-156 and SL-Note-2002-030 AP (2002).
- [22] H. Tsutsui, CERN LHC Project Note 327 (2003).
- [23] F. Caspers, A. Mostacci, H. Tsutsui, CERN SL-2000-071 AP (2000).
- [24] G. Nassibian, F. Sacherer, CERN ISR-TH/77-61 (1977).
- [25] F. Caspers, A. Mostacci, U. Iriso, CERN AB-2003-051 (RF) and PAC'03, Portland (2003).
- [26] H. Tsutsui, CERN SL-Note-2002-034 (2002).
- [27] H. Hahn, *Phys. Rev. ST Accel. Beams* 7, 103501 (2004).
- [28] A. Mostacci, L. Palumbo, B. Spataro et al, NIM A517 (2004), p.19.
- [29] D. Alesini, B. Gagliardo, A. Mostacci, L. Palumbo et al., "Electromagnetic simulations and RF measurements results of an ultra-short bunch length monitor", EPAC'02, Paris (2002).
- [30] D. Alesini, C. D'Alessio, A. Mostacci, L. Palumbo, B. Spataro et al., "Study of a low impedance beam position monitor for short bunches", PAC'03, Portland, (2003).
- [31] R. Rimmer, M. Tinger in *Handbook of Accelerator Physics and Engineering*, A. Chao and M. Tinger (editors), World Scientific, Singapore (1998), p.403.
- [32] T.P. Wangler, *Principles of RF Linear Accelerator*, John Wiley and Sons Inc., Canada (1998).
- [33] F. Caspers, G. Dome, CERN SPS/85-46 ARF (1984).
- [34] A. Bacci, M. Migliorati, L. Palumbo, B. Spataro, INFN LNF 03/008(R) (2003).
- [35] International Organization for Standardization et al., *Guide to the expression of uncertainty in measurement*, ISO, Switzerland (1995).